Yu, Y., Liu, B., Wang, Y. and Cheng, Q. S. (2022) Automated diplexer design with key performance indicator-based objectives. IEEE Microwave and Wireless Components Letters, (doi: 10.1109/LMWC.2022.3150312).

There may be differences between this version and the published version. You are advised to consult the publisher's version if you wish to cite from it.

https://eprints.gla.ac.uk/265211/

Deposited on: 11 February 2022

Enlighten – Research publications by members of the University of Glasgow
https://eprints.gla.ac.uk

Automated Diplexer Design with Key Performance Indicator-Based Objectives

Yang Yu, *Student Member, IEEE,* Bo Liu, *Senior Member, IEEE,* Yi Wang, *Senior Member, IEEE,* Qingsha S. Cheng, *Senior Member, IEEE*

***Abstract*—Microwave diplexers are often designed iteratively via manual channel-by-channel or resonator-by-resonator local optimization procedures due to high dimensionality in design variables and the complexity of structures. A one-off automated diplexer optimization method is yet to be developed. To achieve this, other than improved optimizers, an effective objective function is critical to allow optimizers to find desired designs. This paper realizes automated diplexer design by proposing key performance indicator (KPI)-based objectives. The KPIs are extracted from S-parameter responses. An all-resonator diplexer with 22 variables and a Tee-junction diplexer with 23 variables are designed using the proposed method via one-off optimization, showing 100% and 80% success rates, respectively.**

***Index Terms*—Microwave diplexers, key performance indicators, optimization, objective function.**

I. Introduction

MICROWAVE diplexers are three-port filtering components widely used in satellite and front-end of base stations [1]. Given a topology and an initial design, diplexer design aims to obtain optimal geometric parameters satisfying predefined design specifications [2]. Although analytical design methods are available, they are limited to specific types of channel filters or junctions [3]-[6]. Electromagnetic (EM) simulation-based optimization methods have more generality. However, with a large number of design variables, diplexers are often optimized iteratively via manual channel-by-channel or resonator-by-resonator process using local optimizers [7]-[8]. Designers' experience is essential for dividing the diplexer, formulating each sub-optimization task, as well as guiding each optimization task when the optimizer sticks in local optima.

Automated diplexer design, in contrast, has the following characteristics: (1) only requires an initial design and can obtain the successful final design by pressing one button, and (2) is general to most kinds of structures. Such a diplexer design method is promising due to replacing designers' time with computing resources. Many diplexers can be automatically designed in parallel, using a short time on average and almost zero designer's effort.

For automated diplexer design, a global optimizer is essential considering the highly multimodal design landscape [9] and the number of design variables. A recent surrogate model-assisted evolutionary algorithm for filter optimization (SMEAFO) [8] is employed to carry out global optimization in this work. Another essential element is the objective function (OF), which is what this research focuses on.

The magnitude of S-parameters (e.g., $\max(|S_{11}|)$) within a frequency range is arguably the most widely used OF, but it leads to a complex design landscape [9], posting challenges to optimizers. Another OF using the difference between the extracted coupling matrix (CM) of a candidate design and the ideal CM shows effectiveness in some diplexer cases [10]. However, the main problem of the CM extraction is its low success rate for candidate designs with poor responses, and it is unable to deal with all-resonator diplexers [11]. Another similar OF employs the group delay of the extracted CM to match with the theoretical group delay. This OF requires multiple ad-hoc procedures which depend on designers' experience [12]. A new cognition-driven filter EM optimization method [13]-[15] uses feature zeros to construct OF. The weights to filter poles and return loss are adjusted at different optimization stages, showing clear advantages in smoothing the design landscape. The feature-based OFs have been also widely applied in antenna and other microwave components [16]-[20].

The above OFs are successful but mainly focus on procedure-based diplexer design. For one-off automated design, on the other hand, correctly identifying high potential designs in the optimization process (e.g., responses with good bandwidths and return losses but center frequencies are shifted) is a new requirement. Hence, an OF focusing on this aspect is proposed, called key performance indicator (KPI)-based OF. Automated diplexer design is therefore realized.

II. Performance Extraction and Objective Function

Microwave diplexer design can be formulated as an optimization problem:

$$\boldsymbol{x}_{opt} = \arg\min_{\boldsymbol{x}} U(\boldsymbol{R}(\boldsymbol{x})) \tag{1}$$

where $\boldsymbol{R}(\boldsymbol{x})$ shows the KPIs of a candidate design $\boldsymbol{x} = [x_1,\ldots x_n]^T$. $U(\boldsymbol{R}(\boldsymbol{x}))$ represents the OF using the KPIs. $\boldsymbol{x}_{opt}$ denotes the optimal design. The OF construction process is shown in Fig. 1. In our proposed OF, the KPIs include (1) the return loss, P_R, the center frequency P_C, and the bandwidth P_B of each channel,

Manuscript received September 3, 2021. (Corresponding authors: B. Liu and Q. S. Cheng) This work is partially supported by the UK Engineering and Physical Science Research Council under grant EP/S013113/1 and EP/M013529/1, and also by the National Natural Science Foundation of China Grant 62071211 and the University Key Research Project of Guangdong Province under Grant 2018KZDXM063.

Y. Yu and Q. S. Cheng are with the Dept. of Electrical and Electronic Engineering, Southern University of Science and Technology, Shenzhen, 518055, P.R.China. (emails: issacyu@live.cn, chengqs@sustech.edu.cn).

B. Liu is with James Watt School of Engineering, University of Glasgow, Glasgow, Scotland. G12 8QQ, U.K. (e-mail: bo.liu@glasgow.ac.uk).

Y. Yu, and Y. Wang are with the School of Electrical, Electronic and System Engineering, University of Birmingham, Birmingham B15 2TT, U.K. (e-mails: yxy726@student.bham.ac.uk, y.wang.1@bham.ac.uk).

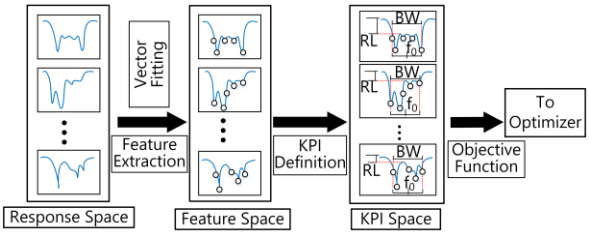

Fig. 1. The OF construction process.

which are extracted from the S_{11} response, (2) the stopband rejection P_S (or isolation between channels P_I), which are described by the magnitudes of S_{21} and S_{31} response, and (3) the frequency locations of transmission zeros P_T, if any.

1) Extraction of frequency locations of reflection zeros (RZs)

Before OF construction, all the RZ frequency locations of the two channels are extracted from S_{11} response. To accurately identify them, a vector fitting technique [21] is employed. It adopts a rational polynomial to fit the S_{11} curve. When the rational polynomial is perfectly fitted with the S_{11} curve, the poles and zeros of the fitted polynomial would accurately approximate those of S_{11}. This method has been successfully used for microwave filter design [22]-[23]. Fig. 2(b) shows a diplexer with all the 10 RZs correctly identified.

2) Extraction of bandwidths (BWs): P_B

To define BW, there are two different situations: (1) When S_{11} values of all RZs in a channel approach or are lower than the desired level (i.e., −20 dB), BW can be directly identified. (2) If any RZs do not reach the specified level, the BW will be defined based on the extracted RZs, namely $P_B = |f_{rz.N} - f_{rz.1}| + \Delta B$, where $f_{rz.N}$ and $f_{rz.1}$ are the highest and lowest RZ frequency locations in one channel as shown in Fig. 2(a). $\Delta B = |B - B_Z|$, defined by the ideal response of the optimal CM.

3) Extraction of return loss: P_R

The RL has different definitions based on the RZ locations:

$$P_R(\boldsymbol{x}) = \begin{cases} max\left(\left|S_{11}\left(\boldsymbol{x}, \left[f_{rz,1}, f_{rz,N}\right]\right)\right|\right) & \forall f_{rz,i}\ (i=1,\ldots,N) \in \left[f_L, f_U\right] \\ max\left(\left|S_{11}\left(\boldsymbol{x}, \left[f_L, f_U\right]\right)\right|\right) & \exists f_{rz,i} (i=1,\ldots,N) \notin \left[f_L, f_U\right] \end{cases} \quad (2)$$

where $[f_{rz,1}, f_{rz,n}]$ is the frequency range between the lowest and highest RZs. $[f_L, f_U]$ is the specified frequency range of the passband of one channel. The first equation in (2) means that all RZs of one channel are within the passband while the other means that at least one RZ exists outside the specified passband.

4) Extraction of the center frequency (P_C) of each channel

The center frequency is defined as $P_C(\boldsymbol{x}) = (f_{rz.1} + f_{rz.N})/2$, where $f_{rz.N}$ and $f_{rz.1}$ are the highest and lowest RZ frequency locations in one channel as shown in Fig. 2(a).

Advantages of the above KPIs are: (1) When the order of the diplexer is high, the S_{11} response is very steep at the passband edges (e.g., Fig. 2(a)) and a minor frequency shift could make a good quality candidate design shows bad max($|S_{11}|$) value. Such good potential designs can still be identified to support correct convergence with the KPI-based OF due to the return loss P_R definition. (2) A kind of wrong design, which often appears in diplexer optimization, is the one with RZs outside of the passband (e.g., Fig. 2(b)). In contrast with the OF based on

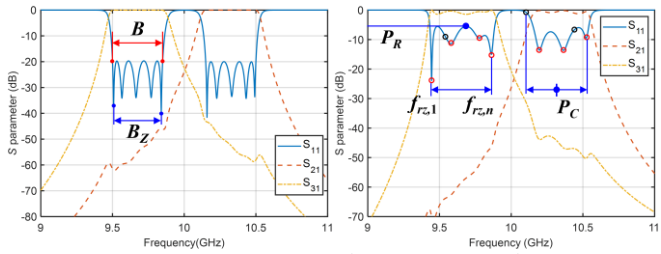

Fig. 2 (a) The S-parameter response of the optimal CM for example 1 in Section III. (b) A typical response in the optimization of the same diplexer.

S-parameter magnitude that is powerless to them, such design is penalized by the P_B. In this case, P_R in (2) does not have to consider the steep S_{11} passband edges.

The KPI-based OF is formulated as

$$F_d(\boldsymbol{x}) = \sum_{j=1}^{n} \beta_j \left[\left| \min\left(P_j(\boldsymbol{x}) - (P_j^S - \Delta_j^{LB}), 0\right) \right| + \max\left(P_j(\boldsymbol{x}) - (P_j^S + \Delta_j^{UB}), 0\right) \right] \quad (3)$$

where $P_j(\boldsymbol{x}) \in \{P_B(\boldsymbol{x}), P_R(\boldsymbol{x}), P_C(\boldsymbol{x}), P_T(\boldsymbol{x}), \ldots\}$ represents the j^{th} extracted KPI value at design $\boldsymbol{x}$, and P_j^S is the corresponding requirement from the design specifications. Δ_j^{UB} and Δ_j^{LB} are the upper and lower acceptable tolerances (e.g., a slight frequency or bandwidth deviation, which may be handled in tuning) for jth KPI. The weighting factors (β_1, ..., β_n) are set such that the KPIs' values are comparable.

III. Application Examples

The first example is a 10th order all-resonator waveguide diplexer shown in Fig. 3. The diplexer contains 22 variables: $\boldsymbol{x} = [l_1, \ldots, l_{10}, k_1, \ldots, k_9, q_1, \ldots, q_3]$. The passbands of the diplexer are 9.5-9.85 GHz and 10.15-10.5 GHz and return losses for two channels are 20dB. Then, the diplexer's target KPIs with tolerances are defined as: $P_R^S \in [20 - 1, 20 + 2]$ (dB); $P_B^S \in [0.35 - 0.02, 0.35 + 0.02]$ (GHz); $P_{C_1}^S \in [9.675 - 0.035, 9.675 + 0.035]$ (GHz), $P_{C2}^S \in [10.325 - 0.035, 10.325 + 0.035]$ (GHz). The initial design for the diplexer is $\boldsymbol{x}_0$ = [14.39, 16.12, 17.3, 17.45, 17.22, 15.46, 18.95, 19.41, 19.18, 17.2, 10.47, 10.76, 6.8, 9.76, 7.51, 11.19, 7.30, 10.11, 8.06, 12.77, 11.08, 11.73], which is obtained from the CM using the classical design curve method [24]-[25]. Our setting for weighting factor is $\beta_1 = 1$, $\beta_2 = 500$, and $\beta_3 = 100$ corresponding to P_R, P_B, and P_C. The simulated responses of the initial design are shown in Fig. 3 (dash lines), and the OF value is 36.8.

The second example is an 8th order Ku-band Tee-junction diplexer shown in Fig. 4. The diplexer has 23 variables: $\boldsymbol{x}^T = [l_1, \ldots, l_8, d_1, \ldots, d_8, w_1, \ldots, w_4, l_{01}, l_{02}, l_{ins}]^T$. The design KPIs with tolerances are defined as: $P_R^S \in [20 - 1, 20 + 2]$ (dB); $P_B^S \in [0.25 - 0.01, 0.25 + 0.01]$ (GHz); $P_{C_1}^S \in [12.625 - 0.025, 12.625 + 0.025]$ (GHz), $P_{C2}^S \in [13.125 - 0.025, 13.125 + 0.025]$ (GHz); $P_I > 55$ (dB). The initial design is obtained from CM are $\boldsymbol{x}_0$= [15.19, 16.65, 16.6, 15.0, 13.75, 15.57, 15.68, 14.32, 5.77, 7.04, 5.65, 7.46, 5.37, 6.75, 0.0487, 7.15, 8.42, 8.41, 8.21, 8.03, 16.69, 16.76, 7.64]. The simulated S-parameter responses for the initial design are shown in Fig. 4 (dash lines) and the OF value is 100.79. Our setting for weighting factor in this example

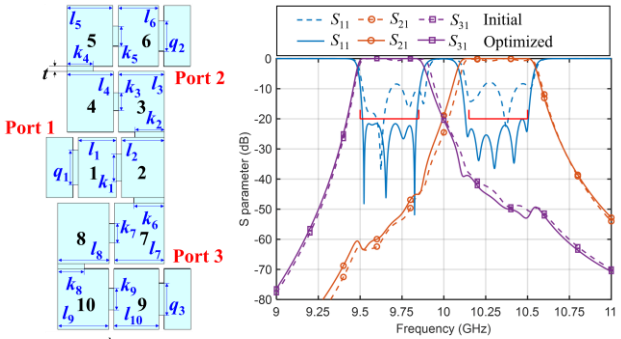

Fig. 3. A 10th order waveguide diplexer and performance of the optimal design. $l_1, \ldots, l_{10}$ are the lengths of the resonators, $d_1, \ldots, d_9$ are the iris widths of the mutual couplings, $w_1, \ldots, w_3$ are the iris widths of the external port couplings. The thickness t of all irises is equal to 2 mm.

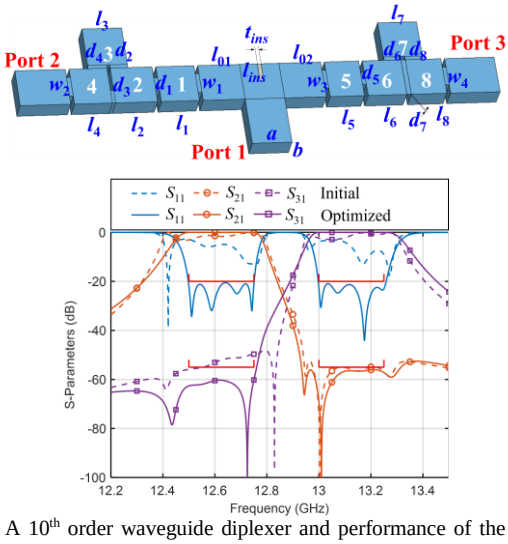

Fig. 4. A 10th order waveguide diplexer and performance of the optimal design. l_{ins} is the length of the metal ridge. The thickness t of all irises and t_{ins} are equal to 1.5 mm. a = 15.799 and b = 7.899 (mm) are standard dimensional values for the WR62 waveguide.

is $\beta_1 = 1$, $\beta_2 = 500$, $\beta_3 = 100$, and $\beta_4 = 1$ corresponding to P_R, P_B, P_C, and P_I.

Five runs are carried out for each diplexer, where SMEAFO [9] is used as the optimizer. The design parameters x and KPIs are involved in the surrogate modeling. On average, example 1 takes 100 hours (1210 EM simulations), and example 2 takes 125 hours (1418 EM simulation) using a laptop computer with an Intel i7-7700HQ 1.8 GHz CPU and 16 GB RAM. No parallel computing is used. The results are shown in Table I. The responses of typical solutions are shown in Fig. 3 and 4. Both OF values achieve 0 (i.e., specifications are met) finally.

The proposed OF are compared with max(|S11|)-based OF using the same optimizer, SMEAFO. Also, some commercial tools in CST studio suite [26], filter designer 3D with CM-difference-based OF, and trust-region framework (TRF) with max(|S11|)-based OF are compared with the same initial design. Success rate means the percentage of successful runs (i.e., meet the specifications) out of total 5 runs. From Table II, only for the proposed OF, 100% and 80% success rates are obtained for the two diplexers, respectively, while for other OFs, the results are far from satisfactory using the same computing budget. The max(|S11|)-based OF with SMEAFO can still succeed but often costs 2 times EM simulations than

TABLE I
PERFORMANCE FUNCTION VALUES FOR TWO DIPLEXER EXAMPLES

Example 1	Spec.	1st	2nd	3rd	4th	5th
P_{R1} (dB)	20	21.60	20.29	19.09	20.20	21.56
P_{R2} (dB)	20	21.38	20.55	19.86	19.02	20.06
P_{B1} (GHz)	0.35	0.33	0.33	0.33	0.33	0.33
P_{B2} (GHz)	0.35	0.36	0.33	0.34	0.33	0.37
P_{C1} (GHz)	9.675	9.708	9.694	9.691	9.704	9.674
P_{C2} (GHz)	10.325	10.316	10.320	10.348	10.337	10.318
Example 2	Spec.	1st	2nd	3rd	4th	5th
P_{R1} (dB)	>20	20.41	20.04	19.91	20.37	20.47
P_{R1}(dB)	>20	20.56	19.94	20.83	19.51	7.11
P_{B1} GHz)	0.25	0.25	0.25	0.25	0.26	0.24
P_{B2} GHz)	0.25	0.26	0.25	0.26	0.26	0.23
P_{C1} (GHz)	12.625	12.626	12.622	12.623	12.629	12.59
P_{C2} (GHz)	13.125	13.128	13.122	13.123	13.122	13.11
P_{I1} (dB)	>55	57.27	55.14	55.44	57.79	54.99
P_{I2} (dB)	>55	56.25	56.46	55.64	55.97	60.42

*The Spec. denotes specifications, IS is extracted isolation performance.

TABLE II
COMPARISONS BETWEEN THE PROPOSED OF AND REFERENCE METHODS

Example 1	Spec.	KPIs+ SMEAFO	S-par+ SMEAFO	S-par + TRF	CM difference
Success rate		100%	0%	N.A.	N.A.
P_{R1} (dB)	20	20.6	15.30	19.43	N.A.
P_{R2} (dB)	20	20.2	19.54	6.89	N.A.
P_{B1} (GHz)	0.35	0.33	0.34	0.36	N.A.
P_{B2} (GHz)	0.35	0.34	0.35	0.48	N.A.
P_{C1} (GHz)	9.675	9.694	9.673	9.664	N.A.
P_{C2} (GHz)	10.325	10.328	10.323	10.393	N.A.
Example 2	Spec.	KPIs+ SMEAFO	S-par+ SMEAFO	S-par + TRF	CM difference
Success rate		80%	0%	N.A.	N.A.
P_{R1} (dB)	20	20.2	0	19.1	9.3
P_{R1}(dB)	20	20.2	6.1	1.9	12.4
P_{B1} GHz)	0.25	0.25	0.42	0.25	0.299
P_{B2} GHz)	0.25	0.26	0.33	0.30	0.274
P_{C1} (GHz)	12.625	12.625	12.615	12.627	12.617
P_{C2} (GHz)	13.125	13.124	13.075	12.877	13.130
P_{I1} (dB)	55	56.4	51.76	26.5	61.1
P_{I2} (dB)	55	56.1	55.13	50.1	58.7

Note: Average results are used for SMEAFO-based optimization. Because the reference methods from CST are deterministic, the success rate does not apply to them. Because CM is not able to be extracted for all-resonator diplexer, CM difference-based OF does not apply to example 1.

the performance-based OF. CM difference-based OF does not succeed because it fails to extract CM from poor candidate designs in the optimization. Also, the local optimizer, TRF in CST, is not able to achieve automated diplexer optimization.

IV. CONCLUSION

To the best of our knowledge, this paper firstly realizes automated diplexer design, with the characteristics of fully automated, general to different structures, and high success rate. KPI objectives play an important role to identify high potential solutions that are beyond the capabilities of existing OFs. The effectiveness is demonstrated by the design of two diplexer design examples with 22 and 23 variables, respectively.

REFERENCES

[1] R. J. Cameron, C. M. Kudsia, and R. R. Mansour, "Multiplexer theory and design," *Microwave Filters for Communication Systems: Fundamentals, Design, and Applications*, Wiley, 2018, pp.569-608, ch18.

[2] B. Liu, H. Yang, and M. J. Lancaster, "Synthesis of coupling matrix for diplexers based on a self-Adaptive differential evolution algorithm," *IEEE Trans. Microw. Theory Techn.*, vol. 66, no. 2, pp. 813-821, Feb. 2018.

[3] G. Macchiarella and S. Tamiazzo, "Novel approach to the synthesis of microwave diplexers," *IEEE Trans. Microw. Theory Techn.*, vol. 54, no. 12, pp. 4281–4290, Dec. 2006.

[4] G. L. Matthaei, L. Young, and E. M. T. Jones, Microwave filters, impedance-matching networks, and coupling structures. Norwood, MA: Artech House, 1980, ch. 8.

[5] R. Levy, "Theory of direct-coupled-cavity filters," *IEEE Trans. Microw. Theory Techn.*, vol. 15, no. 6, pp. 340-348, June. 1967.

[6] G. Macchiarella, "An original approach to the design of bandpass cavity filters with multiple couplings," *IEEE Trans. Microw. Theory Tech.*, vol. 45, no. 2, pp. 179–187, Feb. 1997.

[7] S. Cogollos et al., "Efficient Design of Waveguide Manifold Multiplexers Based on Low-Order EM Distributed Models", *IEEE Trans. Microw. Theory Techn.*, vol. 63, no .8, pp. 2540-2549, 2015.

[8] M. Guglielmi, "Simple CAD procedure for microwave filters and multiplexers," *IEEE Trans. Microw. Theory Techn.*, vol. 42, no. 7, pp. 1347-1352, 1994.

[9] B. Liu, H. Yang, and M. J. Lancaster, "Global optimization of microwave filters based on a surrogate model-assisted evolutionary algorithm," *IEEE Trans. Microw. Theory Techn.*, vol. 65, no. 6, pp. 1976–1985, 2017.

[10] X. Wang, Y. Zhang, G. Shen, W. Che, H. Chen, and W. Feng, "Automated optimization of multiplexers based on aggressive space mapping and cauchy method," *2015 International Workshop on Electromagnetics: Applications and Student Innovation Competition (iWEM)*, Hsinchu, 2015, pp. 1-4.

[11] P. Zhao and K. L. Wu, "Circuit model extraction for computer-aided tuning of a coupled-resonator diplexer," *IEEE MTT-S Int. Microw. Symp. Dig.*, Apr. 2015, pp. 1–3.

[12] M. Sharifi Sorkherizi and A. A. Kishk, "Use of group delay of sub-circuits in optimization of wideband large-scale bandpass filters and diplexers," *IEEE Trans. Microw. Theory Techn.*, vol. 65, no. 8, pp. 2893-2905, Aug. 2017.

[13] C. Zhang, F. Feng, V.-M.-R. Gongal-Reddy, Q. J. Zhang, and J. W. Bandler, "Cognition-driven formulation of space mapping for equal-ripple optimization of microwave filters," *IEEE Trans. Microw. Theory Techn.*, vol. 63, no. 7, pp. 2154–2165, 2015.

[14] C. Zhang, F. Feng, Q. Zhang, and J. W. Bandler, "Enhanced cognition-driven formulation of space mapping for equal-ripple optimisation of microwave filters," *IET Microw. Antennas Propag.*, vol. 12, no. 1, pp. 82-91, Jan 2018.

[15] C. Zhang, J. Jin, Z. Zhao, and Q. Zhang, "Cognition-driven formulation of space mapping for reducing gain variation of antennas," *in IEEE MTT-S Int. Conf. Numer. Electromagn. Multiphysics Modeling Opt. (NEMO)*, Reykjavik, Iceland, Aug. 2018, pp. 1-3.

[16] S. Koziel and A. Pietrenko-Dabrowska, "Design-Oriented Computationally-Efficient Feature-Based Surrogate Modelling of Multi-Band Antennas with Nested Kriging," *AEU - International Journal of Electronics and Communications*, vol. 120, no. 7, pp.153202, 2020.

[17] A. Pietrenko-Dabrowska and S. Koziel, "Optimization-based robustness enhancement of compact microwave component designs with response feature regression surrogates," *Knowledge-Based Systems*, vol. 240, 2022.

[18] A. Pietrenko-Dabrowska and S. Koziel, "Design Centering of Compact Microwave Components Using Response Features and Trust Regions," *Energies*, vol. 14 no. 24, pp.:8550, 2021.

[19] A. Pietrenko-Dabrowska and S. Koziel, "Globalized parametric optimization of microwave components by means of response features and inverse metamodels," *Scientific Reports*, vol. 11, pp. 23718, 2021.

[20] A. Pietrenko-Dabrowska and S. Koziel, "Fast Design Closure of Compact Microwave Components by Means of Feature-Based Metamodels," *Electronics*, vol. 10, no. 1, pp:10, 2021.

[21] B. Gustavsen and A. Semlyen, "Rational approximation of frequency domain response by Vector Fitting", *IEEE Trans. Power Del.*, vol. 14, no. 3, pp. 1052-1061, July 1999.

[22] F. Feng, W. Na, W. Liu, S. Yan, L. Zhu, J. Ma, and Q.-J. Zhang, "Multifeature-assisted neuro-transfer function surrogate-based EM optimization exploiting trust-region algorithms for microwave filter design," *IEEE Trans. Microw. Theory Techn.*, vol. 68, no. 2, pp. 531-542, Feb. 2020.

[23] F. Feng, C. Zhang, W. Na, J. Zhang, W. Zhang, and Q. Zhang, "Adaptive Feature Zero Assisted Surrogate-Based EM Optimization for Microwave Filter Design," *IEEE Microw. Wireless Compon. Lett.*, vol. 29, no. 1, pp. 2-4, Jan. 2019.

[24] J. Hong and M. J. Lancaster, *Microstrip filters for RF/microwave applications*. John Wiley & Sons; 2004.

[25] R. J. Cameron, C. M. Kudsia, and R. R. Mansour, "Design and Physical Realization of Coupled Resonator Filters," *Microwave Filters for Communication Systems: Fundamentals, Design, and Applications*, Wiley, 2018, pp.457-484, ch14.

[26] Dassault Systèmes, 64289 Darmstadt, Germany. CST Studio Suite® 2020.